

RESEARCH ARTICLE

Effects of elevated $p\text{CO}_2$ and feeding on net calcification and energy budget of the Mediterranean cold-water coral *Madrepora oculata*

Cornelia Maier^{1,2,*}, Pauline Popp^{1,2}, Nicole Sollfrank^{1,2}, Markus G. Weinbauer^{1,2}, Christian Wild³ and Jean-Pierre Gattuso^{1,2,4}

ABSTRACT

Ocean acidification is a major threat to calcifying marine organisms such as deep-sea cold-water corals (CWCs), but related knowledge is scarce. The aragonite saturation threshold (Ω_a) for calcification, respiration and organic matter fluxes were investigated experimentally in the Mediterranean *Madrepora oculata*. Over 10 weeks, colonies were maintained under two feeding regimes (uptake of 36.75 and 7.46 $\mu\text{mol C polyp}^{-1} \text{ week}^{-1}$) and exposed in 2 week intervals to a consecutively changing air– CO_2 mix ($p\text{CO}_2$) of 400, 1600, 800, 2000 and 400 ppm. There was a significant effect of feeding on calcification at initial ambient $p\text{CO}_2$, while with consecutive $p\text{CO}_2$ treatments, feeding had no effect on calcification. Respiration was not significantly affected by feeding or $p\text{CO}_2$ levels. Coral skeletons started to dissolve at an average Ω_a threshold of 0.92, but recovered and started to calcify again at $\Omega_a \geq 1$. The surplus energy required to counteract dissolution at elevated $p\text{CO}_2$ ($\geq 1600 \mu\text{atm}$) was twice that at ambient $p\text{CO}_2$. Yet, feeding had no mitigating effect at increasing $p\text{CO}_2$ levels. This could be due to the fact that the energy required for calcification is a small fraction (1–3%) of the total metabolic energy demand and corals even under low food conditions might therefore still be able to allocate this small portion of energy to calcification. The response and resistance to ocean acidification are consequently not controlled by feeding in this species, but more likely by chemical reactions at the site of calcification and exchange processes between the calcicoblastic layer and ambient seawater.

KEY WORDS: Scleractinia, Mediterranean Sea, Deep sea, Metabolic energy, Ocean acidification

INTRODUCTION

Ocean acidification has been recognized as a major threat to many calcifying organisms (Jokiel et al., 2008; Kroeker et al., 2013; Orr et al., 2005; Ries, 2011a,b). The rapid shoaling of the aragonite saturation horizon (ASH) of 1–2 m year^{-1} (Feely et al., 2012) is a concern for the maintenance of organisms confined to the deep sea and cold waters at high latitudes where cold-water corals (CWCs) typically thrive. More than 70% of the present CWC communities

will be subject to under-saturated conditions by the end of the century (Guinotte et al., 2006). Thriving in the deep and dark ocean, they lack the photosynthetic algal endosymbionts (zooxanthellae) of their tropical shallow-water congeners and consequently grow slower (Maier et al., 2009). CWC communities consist of a few frame-building scleractinian species that construct large 3-dimensional structures, sustaining high biodiversity in the deep ocean (Roberts et al., 2006). Because of the dependence on a few species and their relatively slow growth, it had initially been postulated that CWC ecosystems would be even more sensitive to ocean acidification than tropical reefs and that the shoaling of the ASH will thus be a major threat to deep-sea CWCs in the near future (Turley et al., 2007). However, a number of studies have since revealed that CWCs can maintain constant skeletal growth over a large CO_2 partial pressure ($p\text{CO}_2$) range, with levels as high as 1000 μatm (Carreiro-Silva et al., 2014; Hennige et al., 2014; Maier et al., 2013b; Movilla et al., 2014), and still maintain positive skeletal growth at a saturation state for aragonite (Ω_a) slightly below 1 (Form and Riebesell, 2012; Hennige et al., 2015; Jantzen et al., 2013; Maier et al., 2009; Thresher et al., 2011).

In the Mediterranean Sea, the branching *Madrepora oculata* is the dominant habitat-forming CWC species typically found at water depths below 200 m. The deep Mediterranean Sea is characterized by relatively constant and high seawater temperatures (12.5–14°C) and high salinity (~38–39) (Freiwald et al., 2009; Tursi et al., 2004). The relatively high total alkalinity (~2600 $\mu\text{mol kg}^{-1}$) results in a high buffering capacity, with more atmospheric CO_2 being absorbed than in the open ocean (CIESM, 2008). This has already affected the pH in the Mediterranean Sea and resulted in an estimated decrease of 0.005–0.06 pH units since pre-industrial times (Palmiéri et al., 2015). It is possible that the decline in pH may have already reduced calcification rates of *M. oculata* in the Mediterranean Sea (Maier et al., 2012), but current research suggests that it will be unaffected by the additional pH decline projected until the end of the century (Maier et al., 2013a, 2012).

To date, it is unknown how CWCs are able to maintain relatively constant rates of calcification under elevated $p\text{CO}_2$. An up-regulation of genes involved in calcification and other key physiological functions as a rapid response to counteract changes in seawater carbonate chemistry have been proposed for tropical corals (Kanievska et al., 2012; Moya et al., 2012, 2015) and recently for the CWC *Desmophyllum dianthus* (Carreiro-Silva et al., 2014). The use of lipid reserves might also help sustain calcification during short-term exposure to elevated $p\text{CO}_2$ (Hennige et al., 2014). Fast calcification is supported in both tropical corals and CWCs by the up-regulation of pH at the tissue–skeleton interface, the calcicoblast, where the calcareous skeleton is laid down (Al-Horani

¹Sorbonne Universités, UPMC Université Paris 06, Observatoire Océanologique de Villefranche, Villefranche-sur-mer 06230, France. ²CNRS-INSU, Laboratoire d’Océanographie de Villefranche, BP 28, Villefranche-sur-mer 06234, France. ³University of Bremen, Faculty of Biology & Chemistry, Leobener Strasse, Bremen D-28359, Germany. ⁴Institute for Sustainable Development and International Relations, Sciences Po, 27 rue Saint Guillaume, Paris F-75007, France.

*Author for correspondence (maier.conny@gmail.com)

 C.M., 0000-0002-2162-0677

et al., 2003; McCulloch et al., 2012). In warm-water corals, this active process is fuelled by energy provided by light-dependent photosynthesis of algal symbionts, which results in a pronounced increase in calciblastic pH during daytime calcification (Al-Horani et al., 2003; Gattuso et al., 1999). The up-regulation in the calciblastic layer is thought to be an energy-requiring process where active ion transport is mediated via ATP (Allemand et al., 2004; McCulloch et al., 2012; Venn et al., 2013). This suggests that corals require more energy to sustain skeletal growth as seawater pH declines.

The aim of the present study was to determine the energy required to up-regulate the calciblastic pH and to establish the threshold of Ω_a where calcification cannot be sustained and the skeleton starts to dissolve. Furthermore, we investigated whether increased food availability might help mitigate the negative effects of elevated $p\text{CO}_2$ on key physiological functions (respiration, calcification). The CWC *M. oculata* was subjected to $p\text{CO}_2$ levels from ambient (400 μatm) to very high $p\text{CO}_2$ (~1700 μatm), corresponding to Ω_a values ranging between 2.3 and 0.6. The carbon supply to the corals, energy and carbon budgets, rates of respiration and calcification as well as the respiratory quotient (RQ) were determined.

MATERIALS AND METHODS

Sampling and experimental set-up

Two small colonies of the CWC *Madrepora oculata* Linnaeus 1758 were collected at 434 m during the ARCADIA cruise (R/V Urania) on 25 March 2010 with a remotely operated vehicle (ROV) from the Bari Canyon, Adriatic Sea (41°17'16", 17°16'38"). Corals were kept at 13°C in a plastic container (1040×640×515 mm) equipped with chilling, filtration and recirculation units. Several weeks prior to experiments, colonies were carefully fragmented and distributed into single vials (4.5×15 cm, inner diameter×height). Maintenance conditions with flow through and aeration to single vials were as described previously (Maier et al., 2013a,b). At the beginning of the experiments, the buoyant and the skeletal dry mass (Davies, 1989), polyp number and surface area were determined. Skeletal surface area was measured using digital photographs taken from two angles of each single coral fragment using the area calculation function of the software CPCe v3.4 (Kohler and Gill, 2006). The two-dimensional projected area was multiplied by π to approximate the cylindrical surface area of the coral branches. Coral fragments weighed on average 2.9 g for both feeding regimes with, respectively, 32.4 or 32.7 polyps and a surface area of 17.5 and 16.6 cm² for the high (HF) and low (LF) feeding groups (Table 1). None of the size variables was significantly different between the two feeding regimes (one-way ANOVA, $P=0.934$ for skeletal mass, $P=0.956$ for polyp number and $P=0.771$ for skeletal surface area).

HF and LF regime

Madrepora oculata were fed with freshly hatched *Artemia salina* nauplii according to two feeding regimes. In the HF regime ($N=13$),

corals were fed daily from Monday to Friday while corals were fed only twice a week in the LF regime ($N=12$). To assess the average food uptake by *M. oculata* throughout the experiment, feeding rates were determined 5 times at 2 week intervals (Table S1, Fig. S1). Corals were left to feed for 21.1 ± 2.2 h (mean±s.d.). Ten sub-samples of Falcon tubes containing *A. salina* nauplii were used to determine initial concentrations of particulate matter, particulate organic carbon (POC) and nitrogen (PON) from which the concentrations derived at the end of the feeding period were subtracted. Five of the Falcon tubes were used to count the initial number of *A. salina* nauplii, which were fixed with Lugol and counted under a binocular microscope. At the end of the incubation, uptake rates were determined by filtering *A. salina* nauplii left over in the vials onto GF/F filters from which the dry mass of particulate matter, and the concentration of POC and PON were measured. The POC and PON concentrations were measured using a CHN analyser (PerkinElmer 2400 Series II CHNS/O Elemental Analyzer) which was calibrated with glycine (32% of carbon and 18.66% of nitrogen).

The actual uptake of *Artemia* nauplii, particulate matter, POC and PON was modelled taking into account dilution by flow through (Eqns 1–6; Fig. S2), using initial and final concentrations under non flow-through incubation (Table S1). Model calculations were based on the assumption that *A. salina* nauplii are diluted linearly and taken up as a function of concentration (Fig. S1, Table S1) using following equations:

$$D_{t+1} = P_t \times (1 - i_D)^t, \quad (1)$$

$$i_D = \text{FT}/n_t, \quad (2)$$

$$F_{t+1} = P_t \times (1 - i_F)^t, \quad (3)$$

$$i_F = \sqrt{P_{\text{end}}/P_0} - 1, \quad (4)$$

$$P_{t+1} = P_t - D_{t+1} - F_{t+1}, \quad (5)$$

$$\text{Hourly uptake} = \sum_{k=1}^{288} F_k \times F_f/24. \quad (6)$$

D_{t+1} is the remaining *A. salina* nauplii POC, taking into account the dilution by overflow for each time increment; i_D is the linear rate of dilution caused by the continuous flow through for each time increment; FT is the continuous flow of seawater in relation to the volume of the vials (here: 32 ml h⁻¹/300 ml); n_t is the number of time steps (here: 12 h⁻¹ for the stepwise approach using 5 min steps); F_{t+1} is the prey (food) taken up at each time step, dependent on the concentration of prey left over after food uptake and dilution due to overflow at each time increment; i_F is the rate of food uptake, following an exponential function taking into account the changes in prey concentration at each time step (due to dilution and feeding); P_t is the POC concentration at the start of each time increment with a known amount of prey provided at t_0 (P_0); P_{end} is the final POC concentration; P_{t+1} is the prey concentration after dilution due to flow through and feeding; the hourly uptake was calculated on the

Table 1. Size of *M. oculata* fragments, net calcification and respiration at ambient $p\text{CO}_2$ and food uptake

FR	<i>N</i>	SDM (g)	Polyp no.	SSA (cm ²)	<i>G</i> (μmol g ⁻¹ h ⁻¹)	<i>R</i> (μmol g ⁻¹ h ⁻¹)	<i>N</i>	POC uptake (μmol g ⁻¹ h ⁻¹)	PON uptake (μmol g ⁻¹ h ⁻¹)
HF	13	2.9±0.5	32.4±3.4	17.5±2.0	0.091±0.027	0.545±0.149	5	0.775±0.195	0.139±0.047
LF	12	2.9±0.5	32.7±13.3	16.6±2.0	0.043±0.025	0.380±0.113	5	0.195±0.044	0.038±0.008

Data are for the high (HF) and low (LF) feeding regime (FR). Initial skeletal dry mass (SDM), polyp number and skeletal surface area (SSA) were determined before the start of experiments. Skeletal growth (*G*) and respiration rates (*R*) of coral fragments were obtained at ambient $p\text{CO}_2$ (from duplicate samples of T_0 and T_5). Particulate organic carbon (POC) and nitrogen (PON) were derived from *A. salina* nauplii uptake for the duration of experiments and for the HF and LF regimes, taking into account dilution due to flow through and prey uptake as a function of prey concentration at a given time. Values are means±s.e.m.

basis of average food uptake over a 1 week feeding period; k is the index of time steps (here: 1 ... 288 for 5 min increments over 24 h; and F_f is the frequency of feeding per week (HF=5/7, LF=2/7).

Adjustment of $p\text{CO}_2$

The carbonate chemistry was changed in five consecutive steps by adjusting the air– CO_2 mix to $T_1=400$ ppm (ambient air, control); $T_2=1600$ ppm; $T_3=800$ ppm; $T_4=2000$ ppm and $T_5=400$ ppm (control). Higher than ambient $p\text{CO}_2$ levels were obtained by mixing ambient air with pure CO_2 using high-precision mass flow controllers (ANALYT MTC GFC17, 0–10 l for air and 0–10 ml for pure CO_2) and an air compressor (Jun-Air OF302-25B), while for ambient $p\text{CO}_2$, ambient air was used only (Maier et al., 2013a,b, 2012). The same colonies were used repeatedly for each $p\text{CO}_2$ treatment, which means each individual coral fragment underwent the consecutive changes in $p\text{CO}_2$ levels with an acclimation period of 2 weeks. This approach allowed us to use a higher replication than a ‘classic’ design with three parallel $p\text{CO}_2$ treatments and two feeding regimes ($2 \times 3 = 6$ treatments), which would have reduced the number of replicates to 4 (26 fragments/6 treatments) instead of the 13 used in the consecutive design (26 fragments/2 feeding regimes). To avoid misinterpretation with respect to changes in the measured parameters that might have occurred over time independent of treatment level, a zig-zag pattern with respect to consecutive changes of $p\text{CO}_2$ was applied, with ambient $p\text{CO}_2$ controls at the start and end of the experiments (Figs 1 and 2).

Determination of carbonate chemistry, net calcification, respiration and total organic carbon

Net calcification (G), respiration (R) and total organic carbon (TOC) dynamics were determined simultaneously from closed-system incubation vials (350 ml). Prior to closed-system incubation, filtered bulk seawater (1 μm micron bags) with respective $p\text{CO}_2$ levels was prepared (T_0) and distributed into four incubation vials with one control (no coral) and three vials with coral samples. The vials were placed in a water bath ($13 \pm 0.1^\circ\text{C}$, mean \pm s.d.) equipped with submersible magnetic stirrers and a magnet, below a grid on which corals were placed. Coral samples and the control were incubated for an average duration of 17.9 ± 0.6 h (mean \pm s.d., $N=45$). Respiration rates were determined using optodes (Presens OXY-4 mini) equipped with polymer optical fibres (POF, Presens) and small sensors (5 mm diameter) placed inside the incubation vials. Respiration rates were determined from the depletion of O_2 during the incubation period, where oxygen consumption curves (% O_2) were established at 30 s intervals and respiration rates are given as $\mu\text{mol O}_2 \text{ g}^{-1}$ skeletal dry mass h^{-1} . An incubation time of 18 h was used, which was long enough to detect measurable changes in total alkalinity (A_T), necessary to determine calcification rates, but did not generate hypoxic conditions. Oxygen saturation averaged $89.5 \pm 9.8\%$ (mean \pm s.d., $N=121$) at the end of the incubation.

From the bulk seawater, control and coral incubation, 125 ml samples were taken to determine A_T and total dissolved inorganic carbon (C_T) as described by Maier et al. (2012). Additionally, pH on the total scale (pH_T) and salinity were determined from samples of bulk seawater using a pH meter (Metrohm, 826 pH mobile) equipped with a glass electrode (Metrohm, electrode plus) and a conductivity meter (Seven Easy, S30). Parameters of the carbonate chemistry were calculated using A_T , C_T or A_T and pH_T , an average salinity of 38.21 ± 0.26 (mean \pm s.d., $N=45$) and a temperature of $13.6 \pm 0.16^\circ\text{C}$ (mean \pm s.d., $N=45$) using the R software package seacarb (v2.4, <http://CRAN.R-project.org/package=seacarb>). The

carbonate chemistry of the last coral incubation at ambient $p\text{CO}_2$ was not determined because of missing C_T samples, but it was assumed that the offset of parameters of the carbonate chemistry between the control and coral incubation was similar to that of the first ambient $p\text{CO}_2$ (Fig. 1).

Net calcification (G) was calculated from changes in A_T for an estimated 5% increase in A_T due to nutrient excretion (Maier et al., 2013b), as follows:

$$G = -2 \times (\Delta A_T + 0.05 \times \Delta A_T). \quad (7)$$

TOC was determined from 20 ml sub-samples taken with a sterile syringe pre-rinsed with 5 ml sample water and transferred to glass vials, cleaned overnight in 10% hydrochloric acid, rinsed 3 times with Milli-Q water and combusted at 450°C for 4 h. Samples were acidified with 20 μl of 85% phosphoric acid and stored at 4°C pending analysis. Analysis was conducted by high catalytic oxidation with a Shimadzu TOC-VCPH analyser [maximum CV $< 1.5\%$, i.e. $\pm 1 \mu\text{mol C l}^{-1}$, referenced by the consensus

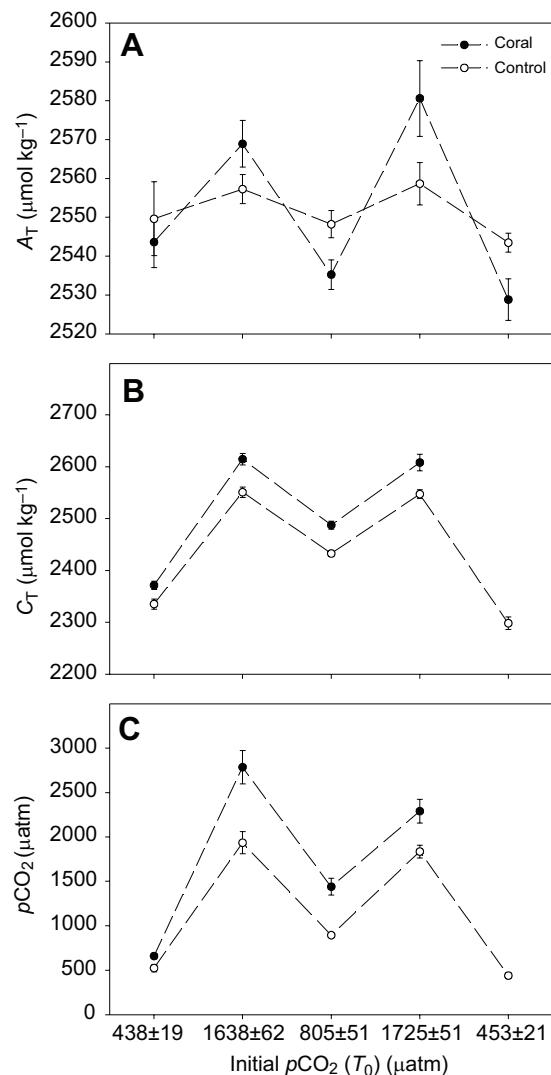


Fig. 1. Parameters of the carbonate chemistry for consecutive 2 week changes in $p\text{CO}_2$ for control and coral incubations. (A) Total alkalinity (A_T), (B) total dissolved inorganic carbon (C_T) and (C) $p\text{CO}_2$ dynamics under high and low feeding regimes (HF and LF). Means \pm s.e.m.; control, $N=9$; coral, $N=25$.

reference materials (CRM) of the Hansell Research Laboratory, USA].

Calculation of the RQ

The RQ was obtained by dividing the amount of CO₂ released (calculated from changes in C_T available for T₁–T₃ and G, taking into account that 1 mol of CaCO₃ precipitated reduces C_T by 1 mol) by the amount of O₂ consumed (R) using the following equations:

$$\text{CO}_2 \text{ respired} = \Delta C_T + G, \quad (8)$$

$$\text{RQ} = \text{CO}_2 \text{ released/O}_2 \text{ consumed} = \text{CO}_2 \text{ released/R}. \quad (9)$$

Up-regulation of aragonite saturation state in the calcicoblast and energy requirements

The up-regulation of the calcicoblast aragonite saturation state (Ω_{CF}), energy requirements for calcification [$E(G)$], surplus energy required for up-regulation of Ω_{CF} [$E(\Delta G)$] and energy equivalents for aerobic respiration [$E(R)$] were calculated for the experimental pCO₂ and Ω_a levels (Table 2) using the following equations:

$$\text{for } G > 1 : \Omega_{CF} = \sqrt[n_c]{G/k_c} + 1, \quad (10)$$

$$\text{for } G < 1 : \Omega_{CF} = 1 - \sqrt[n_d]{-G/k_d}, \quad (11)$$

$$\Delta\Omega = \Omega_{CF} - \Omega_a, \quad (12)$$

$$\text{for } \Omega_a > 1 : G_{sw} = k_c \times (\Omega_a - 1)^{n_c}, \quad (13)$$

$$\text{for } \Omega_a < 1 : G_{sw} = -k_d \times (1 - \Omega_a)^{n_d}, \quad (14)$$

$$\Delta G = G - G_{sw}, \quad (15)$$

$$E(G) = G \times 30,500/2, \quad (16)$$

$$E(\Delta G) = \Delta G \times 30,500/2, \quad (17)$$

$$E(R) = R \times 37,560 \times 12, \quad (18)$$

where Ω_{CF} is the saturation state of aragonite in the calcifying fluid, k_c and k_d are the rate law constants and n_c and n_d are the order of reaction for aragonite for positive calcification or dissolution, respectively. For calcification, $k_c = -0.0177T^2 + 1.47T + 14.9$ and $n_c = 0.0628T + 0.0985$ (Burton and Walter, 1987); for negative calcification (dissolution), no empirical relationship with temperature has been determined, so values of $n_d = 2.5$ and $\log k_d = 2.99$ and 3.39 ($\mu\text{mol m}^{-2} \text{h}^{-1}$) determined at 25°C for zooxanthellate corals *Acropora* and *Fungia*, respectively, were used (Walter and Morse, 1985). G is the measured calcification/dissolution rate, G_{sw} is the rate of calcification or dissolution expected at ambient Ω_a and ΔG is the difference between measured and expected calcification/dissolution rates, all normalized to $\mu\text{mol m}^{-2} \text{h}^{-1}$.

$E(G)$ and $E(\Delta G)$ ($\text{mJ m}^{-2} \text{h}^{-1}$) are the energy required for calcification [$E(G)$] and up-regulation of calcicoblastic pH [$E(\Delta G)$], assuming that 1 mol of ATP or 30.5 J are required for the transport of 2 mol of Ca²⁺ to the site of calcification (McConnaughey and Whelan, 1997). For the energy demand of carbon respiration [$E(R)$], an energy equivalent of 37.56 J mg⁻¹ was used. As RQ values were highly variable (Fig. 4A), a value of 1 was used. This might be a conservative estimation for energy demand with respect to carbon respiration (Fig. 4A). All calculations were based on data normalized to $\text{m}^{-2} \text{h}^{-1}$ from conversion of mass to surface area as determined for coral fragments used in the two feeding regimes (Table 1).

Statistical analysis

Physiological parameters were analysed statistically using the software STATISTICA (v7.0, StatSoft Inc. 2004) and illustrated

using the software package SigmaPlot® (v6.0, SPSS Inc. 2000). The experimental design is a repeated measures design with consecutive changes of pCO₂ and two independent groups for feeding; a repeated measures ANOVA was used with pCO₂ level as the repeated variable and HF and LF as the independent factor. Mauchly's test of sphericity was met for calcification ($P=0.26$), but not for the other variables measured. For *post hoc* comparisons of calcification, the least-significance difference (LSD) test was used (Table S2). For other physiological parameters (respiration, RQ and TOC), several non-parametric tests were conducted (Mann–Whitney U -test, Friedman test,

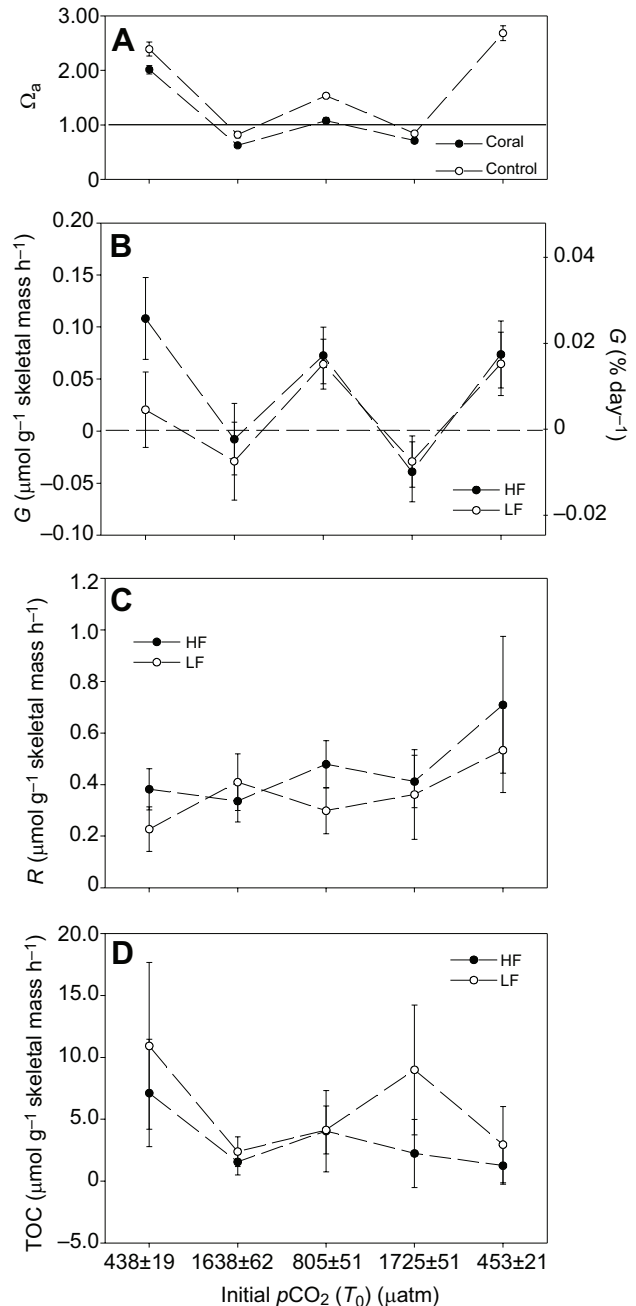


Fig. 2. Physiological response of *M. oculata* to consecutive changes in pCO₂ and Ω_a . (A) Aragonite saturation (Ω_a) calculated from A_T and C_T for control and coral incubation, and (B) net calcification (G), (C) respiration (R) and (D) total organic carbon (TOC) dynamics under HF and LF regimes. Values are means \pm s.e.m.

Table 2. Up-regulation of aragonite saturation state in the calicoblast and energy requirements

$p\text{CO}_2$ (μatm)	FR	Temp. ($^{\circ}\text{C}$)	Ω_a	n_c, n_d	k_c, k_d	R ($\mu\text{mol m}^{-2} \text{h}^{-1}$)	G ($\mu\text{mol m}^{-2} \text{h}^{-1}$)	$G(\Omega_a)$ ($\mu\text{mol m}^{-2} \text{h}^{-1}$)	ΔG ($\mu\text{mol m}^{-2} \text{h}^{-1}$)	Ω_{CF}	$\Delta\Omega_{\text{CF}}$	$E(G)$ ($\text{mJ m}^{-2} \text{h}^{-1}$)	$E(\Delta G)$ ($\text{mJ m}^{-2} \text{h}^{-1}$)	$E(R)$ ($\text{mJ m}^{-2} \text{h}^{-1}$)
438	HF	13.46	1.92	0.94	31.48	639.7	181.3	29.1	152.2	7.10	5.18	2.76	1.21	288.3
	LF	13.52	2.11	0.95	31.54	390.4	35.4	34.8	0.6	2.19	0.08	0.54	0.01	176.0
1638	HF	13.62	0.63	2.50	977	558.7	-12.8	-81.4	68.6	0.82	0.19	-0.19	1.04	251.8
	LF	13.56	0.62	2.50	977	699.4	-49.5	-87.0	37.5	0.70	0.08	-0.75	0.57	315.2
805	HF	13.59	1.00	0.95	31.60	801.6	121.7	0.0	121.7	5.05	4.05	1.85	1.85	361.3
	LF	13.46	1.17	0.94	31.48	515.8	110.9	5.9	105.0	4.73	3.56	1.69	1.60	232.5
1725	HF	13.65	0.71	2.50	977	681.5	-65.6	-44.3	-21.4	0.66	-0.05	-1.00	-0.32	307.1
	LF	13.63	0.71	2.50	977	689.9	-51.6	-44.3	-7.4	0.69	-0.02	-0.78	-0.11	311.0
453	HF	13.62	2.30	0.95	31.64	1249.9	122.7	40.6	82.0	5.06	2.76	1.86	1.25	563.4
	LF	13.65	2.30	0.96	31.67	762.0	109.9	40.7	69.2	4.63	2.33	1.67	1.05	343.5

Data are given for: aragonite saturation (Ω_a), the order of reaction (n_c, n_d), the rate law constants (k_c, k_d), respiration rate (R), the calculated theoretical calcification or dissolution (G) for ambient seawater Ω_a [$G(\Omega_a)$] and the difference in calcification rates between theoretical and measured calcification (ΔG) due to up-regulation of calicoblast aragonite saturation state (Ω_{CF}), the difference in calicoblast and seawater aragonite saturation state ($\Delta\Omega_{\text{CF}}$), and the energy required for calcification [$E(G)$], for calcification due to up-regulation against seawater Ω_a [$E(\Delta G)$] and for respiration [$E(R)$]. Calculations are based on Eqns 10–18. For dissolution at a $p\text{CO}_2$ of 1638 and 1725 μatm , two values are given if calculations are based on the rate law constants (k_d), that were empirically derived by Walter and Morse (1985) for two tropical coral species, *Acropora* sp. (standard) and *Fungia* sp. (italic). FR is feeding regime (HF, high feeding; LF, low feeding).

Kruskal–Wallis ANOVA; Table S3). Additionally, a Wilcoxon matched pairs test with pairs of mean TOC values at T_1 – T_5 , was used to test the effect of feeding regime on TOC dynamics. A paired t -test was used for the comparison of parameters of food uptake (feeding rates and POC:PON ratio) conducted 5 times throughout experiments between HF and LF. Values are given as mean \pm s.e.m.

RESULTS

Food uptake

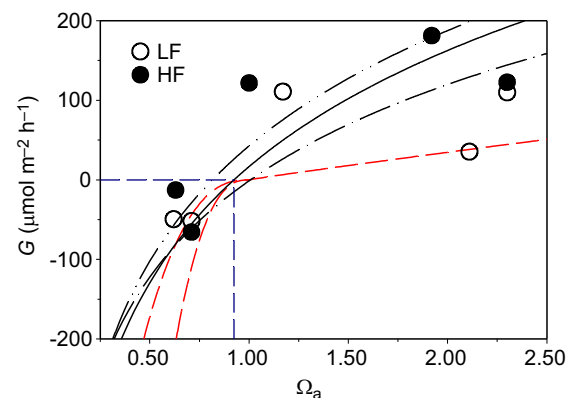
The feeding rate (i_F ; Eqn 4) was determined separately for the HF and LF group and was on average 0.020 ± 0.001 and 0.026 ± 0.002 , respectively. This difference in i_F was significant (paired t -test, $T=3.452$, $P=0.026$, $N=5$) and resulted in relative capture rates of 38.6 ± 2.7 and $48.0\pm 2.1\%$ day $^{-1}$ of food provided for the HF and LF group, respectively (paired t -test for the five feeding assessments, $T=4.187$, $P=0.013$, $N=5$). Mean hourly uptake of POC, taking into account dilution by flow through, prey uptake and weekly feeding times, was on average 0.775 ± 0.195 and 0.195 ± 0.044 $\mu\text{mol g}^{-1}$ skeletal dry mass h^{-1} for the HF and LF group, respectively (Table 1; Fig. S2). The PON uptake was 0.139 ± 0.047 and 0.038 ± 0.008 $\mu\text{mol g}^{-1}$ skeletal dry mass h^{-1} , respectively (Table 1). The ratio of POC:PON taken up by *M. oculata* was higher for the HF compared with the LF group, with values of 6.37 ± 0.67 and 5.09 ± 0.12 , respectively. However, this difference was statistically not significant (paired t -test, $T=-1.76$, $P=0.152$, $N=5$).

Carbonate chemistry

Subsequent 2-weekly treatment levels (T_1 – T_5) for $p\text{CO}_2$ were 438 ± 19 , 1638 ± 62 , 805 ± 51 , 1725 ± 51 and 453 ± 21 μatm . $p\text{CO}_2$ increased during the closed-system incubations to reach 659 ± 30 , 2784 ± 189 , 1440 ± 95 and 2290 ± 133 μatm , respectively, at the end of the incubations. The carbonate chemistry of the last incubation at ambient $p\text{CO}_2$ (T_5) was not determined as a consequence of missing values for C_T or pH_T , but presumably had a similar offset to the first treatment (T_1) at ambient $p\text{CO}_2$. This resulted in Ω_a levels that were well above 1 (2.0–2.4), around 1 or well below 1 (0.6–0.8) (Fig. 2A).

Net calcification

Mean rates of net calcification (G) varied between -0.039 ± 0.029 and 0.108 ± 0.039 $\mu\text{mol g}^{-1}$ skeletal mass h^{-1} depending on $p\text{CO}_2$ level and feeding regime (Fig. 2B). Calcification rates of *M. oculata* as function of Ω_a followed a logarithmic trend and the threshold between calcification and dissolution was 0.92 for Ω_a (Fig. 3; $R=0.763$, $P_{\text{one-tailed}}=0.01$, $N=10$, independent of feeding regime). For the HF and LF regime, the calculated Ω_a threshold was 0.82 and 1.07, respectively (Fig. 3; $R=0.736$, $P_{\text{one-tailed}}=0.07$, $N=5$ and $R=0.866$, $P_{\text{one-tailed}}=0.03$, $N=5$). There was a significant effect of both feeding regime and $p\text{CO}_2$, but no interaction between the two factors (repeated measures ANOVA, feeding regime: $P=0.037$, $p\text{CO}_2$ as repeated factor: $P<0.001$ and $p\text{CO}_2\times$ feeding regime: $P=0.474$). *Post hoc* comparisons revealed that there was only an effect of feeding on calcification for the first incubation at ambient $p\text{CO}_2$ (LSD comparison, $P=0.024$; Table S2). In general, net

**Fig. 3. Mean values of net calcification for the HF and LF regime.**

Logarithmic regression function (solid black line) for net calcification as function of Ω_a used to calculate the threshold level for net calcification pooled for HF ($N=13$) and LF regimes ($N=12$) (horizontal and vertical dashed lines). The grey lines show logarithmic regression functions calculated separately for HF (line, two dots) and LF (line, one dot). Expected net calcification or dissolution rates (red dashed lines) were obtained using equations from Burton and Walter (1987) and Walter and Morse (1985).

calcification was positive and not significantly different between ambient $p\text{CO}_2$ levels (T_1 and T_5) and the $p\text{CO}_2$ level at 800 μatm (T_3), while at very high $p\text{CO}_2$ (1638 and 1725), dissolution set in and calcification was significantly different from that in ambient conditions or 800 μatm (LSD comparison, $P < 0.05$; Table S2). However, *post hoc* comparison within the LF group revealed a less distinct pattern, with calcification rates being only significantly different between a $p\text{CO}_2$ of 1638 μatm (T_2) and 800 μatm (T_3) and between 1638 μatm (T_2) and the last ambient condition (T_5) (LSD comparison, $P < 0.05$; Table S2).

Respiration

There was no treatment effect on respiration (Fig. 2C; Table S3). The overall mean of respiration (data pooled) was $0.431 \pm 0.056 \mu\text{mol g}^{-1}$ skeletal mass h^{-1} ($N=25$). The mean respiration of the HF group was higher than that of the LF group, with $0.481 \pm 0.080 \mu\text{mol g}^{-1}$ skeletal mass h^{-1} ($N=13$) and $0.376 \pm 0.080 \mu\text{mol g}^{-1}$ skeletal mass h^{-1} ($N=12$). This difference was statistically not significant (Table S3).

RQ and carbon budget

The RQ was on average 1.49 ± 0.14 ($N=53$; Fig. 4A). There was no statistically significant effect of feeding or $p\text{CO}_2$, or a significant interaction between the two factors on RQ (Table S3). However, the relative carbon demand from CO_2 respired to POC taken up was significantly different between feeding regimes (Mann–Whitney U -test; Table S3), with a range from 60% to 83% for the HF regime and 180% to 304% for the LF regime (Fig. 4B).

TOC dynamics

There was a high variability in TOC dynamics, ranging from -4.16 to $55.46 \mu\text{mol TOC g}^{-1}$ skeletal mass h^{-1} , with an overall mean of $4.47 \pm 1.13 \mu\text{mol TOC g}^{-1}$ skeletal mass h^{-1} ($N=71$). Because of high variability and several very high outliers, the mean TOC values varied between $1.25 \pm 1.49 \mu\text{mol g}^{-1}$ skeletal mass h^{-1} and $10.93 \pm 6.74 \mu\text{mol g}^{-1}$ skeletal mass h^{-1} (Fig. 2D). The highest mean TOC excretion was observed for the first ambient $p\text{CO}_2$, with values of 7.12 ± 4.33 and $10.93 \pm 6.74 \mu\text{mol g}^{-1}$ skeletal mass h^{-1} for the HF and LF group, respectively. TOC excretion of consecutive $p\text{CO}_2$ treatments was well below that of the initial ambient incubation. Also, median TOC values were generally higher for the LF than for the HF regime, with 1.89 and $-0.12 \mu\text{mol g}^{-1}$ skeletal mass h^{-1} , suggesting that corals of the LF regime excreted more TOC than those of the HF regime. In fact, the slightly negative median value for the HF group indicates that most corals of the HF regime took up TOC. No effect of feeding or $p\text{CO}_2$ was detected using non-parametric tests (Table S3). However, by conducting a Wilcoxon matched pairs test with the means of TOC at T_1 – T_5 , a significant difference in TOC was revealed between feeding regimes ($N=5$, $T=0$; $Z=2.02$, $P=0.043$).

DISCUSSION

The present study confirms earlier findings that net rates of calcification and respiration of *M. oculata* remain relatively unchanged over a large $p\text{CO}_2$ gradient ranging between ambient ($\sim 400 \mu\text{atm}$) and $p\text{CO}_2$ levels projected until the end of the century (Maier et al., 2013a, 2012). A similar resistance to ocean acidification has also been reported for other cold-water scleractinian species (Form and Riebesell, 2012; Jantzen et al., 2013; Lunden et al., 2013; Maier et al., 2013a, 2012; McCulloch et al., 2012; Movilla et al., 2014; Thresher et al., 2011; Hennige et al., 2015; Gori et al., 2016 preprint), while only a few reports are

available where CWC were impacted by increased $p\text{CO}_2$ (Form and Riebesell, 2012; Hennige et al., 2014; Maier et al., 2009). This is, however, the first experimental study, where a threshold level with respect to $p\text{CO}_2$ or Ω_a was reached and skeletal dissolution occurred. After the 2 week exposure to corrosive $p\text{CO}_2$ levels, calcification rates returned to normal when *M. oculata* were subjected to $p\text{CO}_2$ levels of either $\sim 800 \mu\text{atm}$ or ambient. This indicates a strong recovery potential from dissolution due to ocean acidification as had been shown for zooxanthellate corals that had been completely decalcified (Fine and Tchernov, 2007). Higher food uptake had no apparent mitigating effect with respect to the negative impact on calcification at very high $p\text{CO}_2$. Other key physiological parameters – respiration, TOC excretion (or uptake) and RQ – were not significantly related to changes in $p\text{CO}_2$ or feeding regime, which indicates that these metabolic key functions are less sensitive to ocean acidification even when elevated $p\text{CO}_2$ triggered dissolution.

Feeding

Mean C uptake (0.78 and $0.32 \mu\text{mol g}^{-1}$ skeletal mass h^{-1} for HF and LF, respectively) was within the lower range of that reported by Purser et al. (2010) for *Lophelia pertusa* (0.75 – $2.31 \mu\text{mol g}^{-1}$ skeletal mass h^{-1}) and well below that reported by Tsounis et al. (2010) for *M. oculata* ($73 \mu\text{mol C g}^{-1}$ skeletal mass h^{-1}). While corals of the LF regime took up relatively more prey than those of the HF regime, both groups took up a higher percentage of prey with increasing prey concentration (Fig. S1) and, contrary to the findings by Purser et al. (2010), no saturation in food uptake was observed.

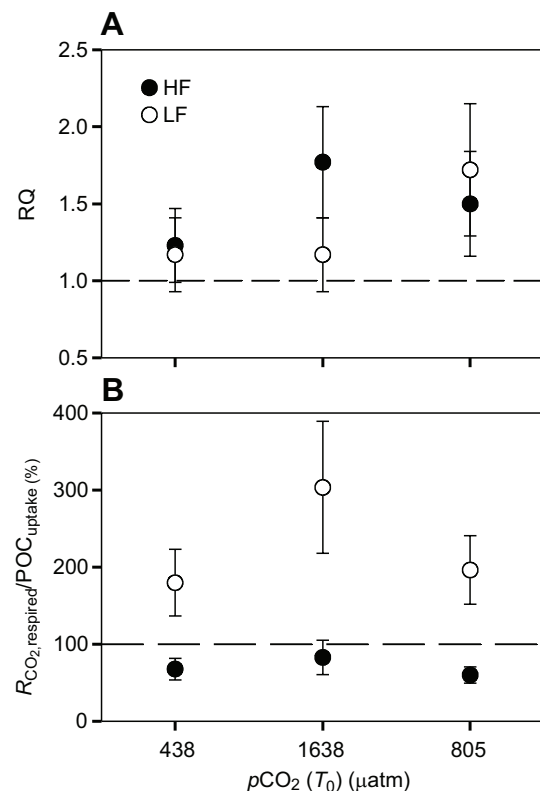


Fig. 4. Metabolic demand of *M. oculata*. (A) Respiratory quotient (RQ). Dashed line indicates RQ=1. (B) Carbon demand for respiration, expressed as CO_2 respired ($R_{\text{CO}_2, \text{ respired}}$) in relation to organic carbon taken up by prey capture ($\text{POC}_{\text{uptake}}$). Dashed line indicates 100%. Values are means \pm s.e.m. ($N=8$ for HF, $N=7$ for LF).

This might indicate that corals, even in the HF regimes, were still below their capture capacity or even starving. However, while the carbon demand for respiration revealed that corals of the LF could not meet the carbon demand by food uptake and were thus slightly starving, corals of the HF regime took up enough prey to meet their respiratory carbon demand (Fig. 4B).

TOC dynamics

The findings of the present and previous studies hint at a dynamic switch between excretion and uptake of TOC (Houlbrèque et al., 2004; Tremblay et al., 2012). Strikingly, corals of the HF group revealed mostly negative TOC values (55%, $N=40$), actually indicating net TOC uptake. This is surprising as TOC uptake has so far only been observed as a consequence of 3 weeks of starvation in the CWC *D. dianthus* (Naumann et al., 2011) and rarely in tropical corals (Houlbrèque et al., 2004; Naumann et al., 2010). Earlier studies reported that high amounts of TOC, dissolved organic carbon (DOC) or POC were excreted by the CWCs *M. oculata*, *L. pertusa* (Maier et al., 2011; Naumann et al., 2013b; Wild et al., 2008; Zetsche et al., 2016) and *D. dianthus* (Naumann et al., 2011). For North Atlantic and Mediterranean *M. oculata*, mean DOC release was 2.57 and 0.53 $\mu\text{mol g}^{-1}$ skeletal mass h^{-1} , respectively (Maier et al., 2011; Naumann et al., 2013b), with the latter corresponding to the overall median values of the present study (0.51 $\mu\text{mol g}^{-1}$ skeletal mass h^{-1}). In the present study, TOC dynamics were measured during closed-system incubation, and no food was provided during that time. As the incubation water had been filtered through 1 μm micron bags, the TOC fraction consisted mainly of DOM, femtoplankton and picoplankton. This is a size fraction that is unlikely to be taken up by active capture, and is more likely to be obtained through passive trapping in the mucus layer.

Function of mucus

The composition and function of coral mucus can greatly vary (Brown and Bythell, 2005; Ducklow and Mitchell, 1979), and corals can reverse their ciliate movement, changing the direction of mucus flow either inward or outward, to or from the coelenteron. This is an important mechanism which allows a switch from food ingestion to a removal of undesired components, such as food remnants, metabolites with high N content (Wild et al., 2008), sediment or other particles (Larsson et al., 2013; Larsson and Purser, 2011; Zetsche et al., 2016). Also, mucus has an important role in fuelling bacterial growth in the coelenteron (Herndl and Velimirov, 1986; Weinbauer et al., 2012) and the close vicinity of the coral environment (Wild et al., 2004a,b, 2008, 2009, 2005). In the light of the diverse role of mucus, a frequent switch between TOC excretion and uptake might be related to the direction of mucus flow transporting mucus-trapped TOC into (uptake) or out of the coelenteron (excretion), where for corals of the HF the more frequently observed TOC uptake might be a consequence of the more frequent food uptake and inward-directed ciliate and mucus movement.

Respiration and net calcification

During the first incubation at ambient $p\text{CO}_2$, respiration and calcification were concomitantly elevated in the HF compared with the LF regime. This might indicate that the two processes are coupled and both depend on the energy provided as suggested earlier (Anthony et al., 2002; Naumann et al., 2011). However, at consecutive $p\text{CO}_2$ levels, net calcification was similar for the HF and LF regimes, while respiration showed opposing trends with respect to $p\text{CO}_2$ and feeding regime: (1) the consecutive 2 week

changes in $p\text{CO}_2$ (or Ω_a) induced an inverse pattern for the two feeding regimes: respiration of the HF group increased or decreased with increasing or decreasing Ω_a , while the opposite was true for the LF regime (Fig. 2A,C); and (2) respiration was about twice as high in the HF as in the LF group at ambient $p\text{CO}_2$ and at a $p\text{CO}_2$ of $\sim 800 \mu\text{atm}$, while it was identical for the two feeding regimes at the very high $p\text{CO}_2$ levels when skeletal dissolution set in (Fig. 2A–C).

Effect of nutrition on metabolic functioning

So far, three studies have addressed the effect of nutrition in relation to calcification and respiration, which revealed several features. Starvation triggers a continuous decline in respiration rates of *L. pertusa* and *D. dianthus* (Larsson et al., 2013; Naumann et al., 2013a). Starvation of *D. dianthus* caused an initial and significant decrease in calcification after 1 week, while starvation for another 2 weeks did not result in further significant reduction of calcification rates (Naumann et al., 2013b). When *L. pertusa* was provided with various concentrations of food over 15 weeks, only small and non-significant changes in respiration were measured, and no effect on calcification occurred, despite the fact that food supply varied by a factor of 7.5 (Larsson et al., 2013). Also, for *M. oculata* (this study) the HF regime only affected the first measurements on calcification, which were taken 2 weeks after the respective feeding regimes had been applied, while during later measurements (4–10 weeks), calcification was independent of feeding regime. This is astonishing as it appears that, while the carbon supply was above the carbon demand in the HF group, the respiratory carbon demand of the LF was not met by the uptake of *A. salina* (Fig. 4B). These different findings therefore suggest that energy allocation to calcification and energy allocation to respiration are largely independent of each other and that these two processes depend not only on the amount of food provided but also on the time scale, the time of last feeding and the regularity of food provided.

Potential contribution of anaerobic oxidation to calcification

The RQ values reported in the present paper, the first in CWCs, are around 1.5. Earlier measurements of RQ in zooxanthellate corals ranged between 0.7 and 1.0 (Gattuso and Jaubert, 1990), which is also the range of values for aerobic metabolism. The high values found in the present study might consequently be due to anaerobic glycolysis driving calcification as suggested by Wooldridge (2013), via the glyoxylate cycle, which was shown to be present in cnidarians (Kondrashov et al., 2006). As RQ is calculated as the number of moles of CO_2 released per mole of O_2 consumed, the lack of O_2 consumption during anaerobic conditions could lead to RQ values higher than 1. Based on this rationale, the contribution of anaerobic oxidation to calcification was calculated to range between 30% and 85%. A complete oxygen depletion close to the calciblastic layer had been shown by micro-electrode profiles during the dark in zooxanthellate corals (Kühl et al., 1995), as well as for the CWC *D. dianthus* (F. Bils, M. A. Peck and C.M., unpublished observation). This, along with the high RQ values of the present study and the molecular evidence for an anaerobic glyoxylate cycle in Cnidaria (Kondrashov et al., 2006) thus support the hypothesis that anaerobic processes might indeed be involved in calcification.

Leakage of ambient seawater into the calciblastic layer

The large range with respect to the contribution of anaerobic oxidation, but also the observed large range in calcification rates

could be explained by a sporadic leakage of ambient seawater into the calicoblast as suggested earlier (Adkins et al., 2003). While oxygen-rich ambient seawater close to the calicoblastic layer would favour aerobic metabolism, the lower ambient pH or Ω_a could slow calcification down. The negative impact on calcification during replenishment of the calicoblastic layer with oxygen-rich, ambient seawater might be partly counteracted by the increased contribution of aerobic oxidation, which is energetically more efficient (Wijgerde et al., 2014). A gradual restoration of gradients of carbonate chemistry between the calicoblast and seawater with a continuous O_2 depletion and increase of the pH and Ω_a in the calicoblast would then gradually favour higher rates of calcification accompanied by an increasing contribution of anaerobic glycolysis. This process would thus act like a see-saw, counterbalancing negative effects of a lower energy efficiency with more favourable conditions for calcification. This hypothesis requires further testing.

Effect of pCO_2 on key physiological processes

This is the first experimental study where a threshold with respect to pCO_2 for CWC calcification was reached and skeletal dissolution set in (Fig. 3). So far, experiments have shown that CWCs can maintain calcification constant over a large pCO_2 gradient (Form and Riebesell, 2012; Hennige et al., 2014; Maier et al., 2013b, 2012; Movilla et al., 2014) and maintain positive skeletal growth even at conditions under-saturated with respect to Ω_a (Form and Riebesell, 2012; Jantzen et al., 2013; Maier et al., 2009; Rodolfo-Metalpa et al., 2015; Thresher et al., 2011). Despite the two thresholds determined for the two feeding regimes, the present study revealed no significant difference in calcification with respect to feeding except at the first ambient pCO_2 , which forced the two regression functions to higher and lower Ω_a threshold values. Still, the given range in thresholds between an Ω_a of 0.8 and 1.1 reflect those observed *in situ* with respect to the distributional limitation of CWCs (Jantzen et al., 2013; Lunden et al., 2013; Thresher et al., 2011). This indicates that the projected decline in ocean pH might be less detrimental than initially thought (Guinotte et al., 2006; Turley et al., 2007), although slowing down of net calcification has been reported under various conditions (Form and Riebesell, 2012; Maier et al., 2009, 2012; Movilla et al., 2014). Recent studies revealed that in the calicoblast the pH up-regulation can greatly differ on a micro-scale (Movilla et al., 2014; Raddatz et al., 2014), which may further explain the observed variable results and threshold values for calcification.

Energy requirements for up-regulation of the calicoblastic pH

There is proxy evidence that the pH of the calicoblast layer is up-regulated (McCulloch et al., 2012), which explains why CWCs are able to calcify relatively fast despite the unfavourable carbonate chemistry of ambient seawater. The up-regulation is an energy-requiring process via active ion transport (Allemand et al., 2004; McCulloch et al., 2012). Hence, when the gradient increases, corals have to invest more energy in calcification to counteract increasingly unfavourable conditions (Cohen and Holcomb, 2009). Therefore, one can expect that more food should favour faster calcification. In the present study, this was only the case after initial changes in food availability (2 weeks), where at the first ambient pCO_2 more food resulted in faster calcification. However, during the subsequent stages (>4 weeks), calcification was independent of feeding. Calculations (Eqns 16–18) revealed that less than 0.5% of energy would be required for calcification in relation to overall respiration in *M. oculata* (Table 2). Also, for

L. pertusa only 3–5% of the available energy is allocated to calcification in comparison to respiration (Larsson et al., 2013), and metabolic carbon contribution to calcification was 1% in relation to that of the tissue pool and respiration for the CWC *L. pertusa* (Mueller et al., 2014). The relatively low energy requirement for up-regulation of Ω_a in the calcifying fluid and the maintenance of relatively high calcification rates might explain the observed resistance to ocean acidification. An increasing gradient of pCO_2 between the calicoblastic space and ambient seawater might consequently be counteracted by allocating relatively small amounts of energy to sustain calcification or delay dissolution. Despite the apparently low surplus energy required to sustain calcification over a large pCO_2 range, the question arises whether this additional allocation of energy to calcification will hamper other physiological functions, such as tissue regeneration (Horwitz and Fine, 2014), reproduction and recruitment as demonstrated for tropical corals (Albright, 2011; Albright and Langdon, 2011; Albright et al., 2008; Crook et al., 2013; Nakamura et al., 2011).

Dissolution rates were calculated using equations established at 25°C, probably over-estimating the calculated dissolution rates and thus the energy allocated to up-regulate calicoblastic pH, as dissolution slows down with decreasing temperature (McCulloch et al., 2012). The energy demand (Table 2) to maintain calcification constant at 800 μatm was in general only 1% of that of respiratory metabolism; however, this is 2 times that required for calcification at ambient pCO_2 . Once the Ω_a drops below 1 and dissolution occurs, the energy required to slow down or counteract dissolution is calculated to be 0.5 to 3 times that at ambient. This may already constitute a limitation with respect to the energy that CWCs can allocate to calcification. However, there is no indication that any surplus energy is allocated to calcification in the HF group to counteract the negative effects at very high pCO_2 . Ultimately, this means that there is a limit with respect to the capacity of a coral to up-regulate its calicoblastic pH, possibly due to a coral's capacity to shelter the calicoblastic space from ambient seawater (Ries, 2011a,b), and surplus energy can consequently not mitigate the detrimental effect on calcification at very high pCO_2 levels.

Acknowledgements

We would like to thank M. Taviani, captain and crew of RV Urania, with special thanks to Maria Berzunza-Sanchez, Cecile Rottier and M. Naumann for coral sampling and maintenance prior to experiments.

Competing interests

The authors declare no competing or financial interests.

Author contributions

Conceptualization: C.M., J.-P.G., M.W.; Methodology: C.M., C.W., P.P., N.S., J.-P.G., M.W.; Formal analysis and investigation: C.M., P.P., N.S.; Writing – original draft preparation: C.M.; Writing – review and editing: C.M., J.-P.G., C.W., M.W., N.S.; Funding acquisition: J.-P.G., M.W., C.M.; Resources: J.-P.G., M.W., C.M.; Supervision: J.-P.G., M.W., C.W., C.M.

Funding

This work was financially supported by the European Commission through a Marie-Curie Fellowship to C.M. (MECCA, project no 220299) and the project COMP via the Prince Albert II of Monaco Foundation. N.S. acknowledges support by the German Academic Exchange Service (Deutscher Akademischer Austauschdienst, DAAD). This work is a contribution to the 'European Project on Ocean Acidification' (EPOCA) which received funding from the European Community's Seventh Framework Programme FP7/2007–2013) under grant agreement no. 211384.

Supplementary information

Supplementary information available online at <http://jeb.biologists.org/lookup/doi/10.1242/jeb.127159.supplemental>

References

- Adkins, J. F., Boyle, E. A., Curry, W. B. and Lutringer, A. (2003). Stable isotopes in deep-sea corals and a new mechanism for “vital effects”. *Geochim. Cosmochim. Acta* **67**, 1129–1143.
- Albright, R. (2011). Reviewing the effects of ocean acidification on sexual reproduction and early life history stages of reef-building corals. *J. Mar. Biol.* **2011**, 473615.
- Albright, R. and Langdon, C. (2011). Ocean acidification impacts multiple early life history processes of the Caribbean coral *Porites astreoides*. *Glob. Change Biol.* **17**, 2478–2487.
- Albright, R., Mason, B. and Langdon, C. (2008). Effect of aragonite saturation state on settlement and post-settlement growth of *Porites astreoides* larvae. *Coral Reefs* **27**, 485–490.
- Al-Horani, F. A., Al-Moghrabi, S. M. and de Beer, D. (2003). The mechanism of calcification and its relation to photosynthesis and respiration in the scleractinian coral *Galaxea fascicularis*. *Mar. Biol.* **142**, 419–426.
- Allemand, D., Ferrier-Pagès, C., Furla, P., Houlbrèque, F., Puverel, S., Reynaud, S., Tambutté, É., Tambutté, S. and Zoccola, D. (2004). Biomineralisation in reef-building corals: from molecular mechanisms to environmental control. *C. R. Palevol.* **3**, 453–467.
- Anthony, K. R. N., Connolly, S. R. and Willis, B. L. (2002). Comparative analysis of energy allocation to tissue and skeletal growth in corals. *Limnol. Oceanogr.* **47**, 1417–1429.
- Brown, B. E. and Bythell, J. C. (2005). Perspectives on mucus secretion in reef corals. *Mar. Ecol. Prog. Ser.* **296**, 291–309.
- Burton, E. A. and Walter, L. M. (1987). Relative precipitation rates of aragonite and Mg calcite from seawater: Temperature or carbonate ion control? *Geology* **15**, 111.
- Carreiro-Silva, M., Cerqueira, T., Godinho, A., Caetano, M., Santos, R. S. and Bettencourt, R. (2014). Molecular mechanisms underlying the physiological responses of the cold-water coral *Desmophyllum dianthus* to ocean acidification. *Coral Reefs* **33**, 465–476.
- CIESM (2008). Impacts of ocean acidification on biological, chemical and physical systems in the Mediterranean and Black Seas. In *CIESM Workshop Monographs*, Vol. 36 (ed. F. Briand), p. 124. Monaco: CIESMA.
- Cohen, A. L. and Holcomb, M. (2009). Why corals care about ocean acidification: uncovering the mechanism. *Oceanography* **22**, 118–127.
- Crook, E. D., Cooper, H., Potts, D. C., Lambert, T. and Paytan, A. (2013). Food availability and pCO₂ impacts on planulation, juvenile survival, and calcification of the azooxanthellate scleractinian coral, *Balanophyllia elegans*. *Biogeosciences* **10**, 7599–7608.
- Davies, P. S. (1989). Short-term growth measurements of corals using an accurate buoyant weighing technique. *Mar. Biol.* **101**, 389–395.
- Ducklow, H. W. and Mitchell, R. (1979). Composition of mucus released by coral reef coelenterates. *Limnol. Oceanogr.* **24**, 706–714.
- Feely, R. A., Sabine, C. L., Byrne, R. H., Millero, F. J., Dickson, A. G., Wanninkhof, R., Murata, A., Miller, L. A. and Greeley, D. (2012). Decadal changes in the aragonite and calcite saturation state of the Pacific Ocean. **26**, GB3001.
- Fine, M. and Tchernov, D. (2007). Scleractinian coral species survive and recover from decalcification. *Science* **315**, 1811.
- Form, A. U. and Riebesell, U. (2012). Acclimation to ocean acidification during long-term CO₂ exposure in the cold-water coral *Lophelia pertusa*. *Glob. Change Biol.* **18**, 843–853.
- Freiwald, A., Beuck, L., Rüggeberg, A., Taviani, M. and Hebbeln, D. (2009). The white coral community in the central Mediterranean Sea revealed by ROV surveys. *Oceanography* **22**, 58–74.
- Gattuso, J.-P. and Jaubert, J. (1990). Effect of light on oxygen and carbon dioxide fluxes and on metabolic quotients measured in situ in a zooxanthellate coral. *Limnol. Oceanogr.* **35**, 1796–1804.
- Gattuso, J.-P., Allemand, D. and Frankignoulle, M. (1999). Photosynthesis and calcification at cellular, organismal and community levels in coral reefs: a review on interactions and control by carbonate chemistry. *Amer. Zool.* **39**, 160–183.
- Gori, A., Ferrier-Pagès, C., Hennige, S. J., Murray, F., Rottier, C., Wicks, L. C. and Roberts, J. M. (2016). Physiological response of the cold-water coral *Desmophyllum dianthus* to thermal stress and ocean acidification. *PeerJ* **4**, e1606. doi:10.7717/peerj.1606
- Guinotte, J. M., Orr, J., Cairns, S., Freiwald, A., Morgan, L. and George, R. (2006). Will human-induced changes in seawater chemistry alter the distribution of deep-sea scleractinian corals? *Front. Ecol. Environ.* **4**, 141–146.
- Hennige, S. J., Wicks, L. C., Kamenos, N. A., Bakker, D. C. E., Findlay, H. S., Dumousseaud, C. and Roberts, J. M. (2014). Short-term metabolic and growth responses of the cold-water coral *Lophelia pertusa* to ocean acidification. *Deep Sea Res. Part 2 Top. Stud. Oceanogr.* **99**, 27–35.
- Hennige, S. J., Wicks, L. C., Kamenos, N. A., Perna, G., Findlay, H. S. and Roberts, J. M. (2015). Hidden impacts of ocean acidification to live and dead coral framework. *Proc. R. Soc. B Biol. Sci.* **282**, 20150990.
- Herndl, G. J. and Velimirov, B. (1986). Microheterotrophic utilization of mucus released by the Mediterranean coral *Cladocora cespitosa*. *Mar. Biol.* **90**, 363–369.
- Horwitz, R. and Fine, M. (2014). High CO₂ detrimentally affects tissue regeneration of Red Sea corals. *Coral Reefs* **33**, 819–829.
- Houlbrèque, F., Tambutté, E., Richard, C. and Ferrier-Pagès, C. (2004). Importance of a micro-diet for scleractinian corals. *Mar. Ecol. Prog. Ser.* **282**, 151–160.
- Jantzen, C., Häussermann, V., Försterra, G., Laudien, J., Ardelan, M., Maier, S. and Richter, C. (2013). Occurrence of a cold-water coral along natural pH gradients (Patagonia, Chile). *Mar. Biol.* **160**, 2597–2607.
- Jokiel, P. L., Rodgers, K. S., Kuffner, I. B., Andersson, A. J., Cox, E. F. and Mackenzie, F. T. (2008). Ocean acidification and calcifying reef organisms: a mesocosm investigation. *Coral Reefs* **27**, 473–483.
- Kaniewska, P., Campbell, P. R., Kline, D. I., Rodriguez-Lanetty, M., Miller, D. J., Dove, S. and Hoegh-Guldberg, O. (2012). Major cellular and physiological impacts of ocean acidification on a reef building coral. *PLoS ONE* **7**, e34659.
- Kohler, K. E. and Gill, S. M. (2006). Coral Point Count with Excel extensions (CPCe): A Visual Basic program for the determination of coral and substrate coverage using random point count methodology. *Comput. Geosci.* **32**, 1259–1269.
- Kondrashov, F. A., Koonin, E. V., Morgunov, I. G., Finogenova, T. V. and Kondrashova, M. N. (2006). Evolution of glyoxylate cycle enzymes in Metazoa: evidence of multiple horizontal transfer events and pseudogene formation. *Biol. Direct* **1**, 31.
- Kroeker, K. J., Kordas, R. L., Crim, R., Hendriks, I. E., Ramajo, L., Singh, G., Duarte, C. and Gattuso, J.-P. (2013). Impacts of ocean acidification on marine organisms: quantifying sensitivities and interaction with warming. *Glob. Change Biol.* **19**, 1884–1896.
- Kühl, M., Cohen, Y., Dalsgaard, T., Jørgensen, B. B. and Revsbech, N. P. (1995). Microenvironment and photosynthesis of zooxanthellae in scleractinian corals studied with microsensors for O₂, pH and light. *Mar. Ecol. Prog. Ser.* **117**, 159–172.
- Larsson, A. I. and Purser, A. (2011). Sedimentation on the cold-water coral *Lophelia pertusa*: Cleaning efficiency from natural sediments and drill cuttings. *Mar. Pollut. Bull.* **62**, 1159–1168.
- Larsson, A. I., Lundälv, T. and van Oevelen, D. (2013). Skeletal growth, respiration rate and fatty acid composition in the cold-water coral *Lophelia pertusa* under varying food conditions. *Mar. Ecol. Prog. Ser.* **483**, 169–184.
- Lunden, J. J., Georgian, S. E. and Cordes, E. E. (2013). Aragonite saturation states at cold-water coral reefs structured by *Lophelia pertusa* in the northern Gulf of Mexico. *Limnol. Oceanogr.* **58**, 354–362.
- Maier, C., Hegeman, J., Weinbauer, M. G. and Gattuso, J.-P. (2009). Calcification of the cold-water coral *Lophelia pertusa* under ambient and reduced pH. *Biogeosciences* **6**, 1671–1680.
- Maier, C., de Kluijver, A., Agis, M., Brussaard, C. P. D., van Duyl, F. C. and Weinbauer, M. G. (2011). Dynamics of nutrients, total organic carbon, prokaryotes and viruses in onboard incubations of cold-water corals. *Biogeosciences* **8**, 2609–2620.
- Maier, C., Watremez, P., Taviani, M., Weinbauer, M. G. and Gattuso, J.-P. (2012). Calcification rates and the effect of ocean acidification on Mediterranean cold-water corals. *Proc. R. Soc. B Biol. Sci.* **279**, 1716–1723.
- Maier, C., Bils, F., Weinbauer, M., Watremez, P., Peck, M. and Gattuso, J.-P. (2013a). Respiration of Mediterranean cold-water corals is not affected by ocean acidification as projected for the end of the century. *Biogeosciences* **10**, 5671–5680.
- Maier, C., Schubert, A., Berzunza Sánchez, M. M., Weinbauer, M. G., Watremez, P. and Gattuso, J.-P. (2013b). End of the century pCO₂ levels do not impact calcification in Mediterranean cold-water corals. *PLoS ONE* **8**, e62655.
- McConnaughey, T. A. and Whelan, J. F. (1997). Calcification generates protons for nutrient and bicarbonate uptake. *Earth Sci. Rev.* **42**, 95–117.
- McCulloch, M., Trotter, J., Montagna, P., Falter, J., Dunbar, R., Freiwald, A., Försterra, G., López Correa, M., Maier, C., Rüggeberg, A. et al. (2012). Resilience of cold-water scleractinian corals to ocean acidification: Boron isotopic systematics of pH and saturation state up-regulation. *Geochim. Cosmochim. Acta* **87**, 21–34.
- Movilla, J., Gori, A., Calvo, E., Orejas, C., López-Sanz, À., Dominguez-Carrió, C., Grinyó, J. and Pelejero, C. (2014). Resistance of two Mediterranean cold-water coral species to low-pH conditions. *Water* **5**, 59–67.
- Moya, A., Huisman, L., Ball, E. E., Hayward, D. C., Grasso, L. C., Chua, C. M., Woo, H. N., Gattuso, J.-P., Forêt, S. and Miller, D. J. (2012). Whole transcriptome analysis of the coral *Acropora millepora* reveals complex responses to CO₂-driven acidification during the initiation of calcification. *Mol. Ecol.* **21**, 2440–2454.
- Moya, A., Huisman, L., Forêt, S., Gattuso, J.-P., Hayward, D. C., Ball, E. E. and Miller, D. J. (2015). Rapid acclimation of juvenile corals to CO₂-mediated acidification by upregulation of heat shock protein and Bcl-2 genes. *Mol. Ecol.* **24**, 438–452.
- Mueller, C. E., Larsson, A. I., Veuger, B., Middelburg, J. J. and van Oevelen, D. (2014). Opportunistic feeding on various organic food sources by the cold-water coral *Lophelia pertusa*. *Biogeosciences* **11**, 123–133.
- Nakamura, M., Ohki, S., Suzuki, A. and Sakai, K. (2011). Coral larvae under ocean acidification: survival, metabolism, and metamorphosis. *PLoS ONE* **6**, e14521.

- Naumann, M. S., Haas, A., Struck, U., Mayr, C., el-Zibdah, M. and Wild, C. (2010). Organic matter release by dominant hermatypic corals of the Northern Red Sea. *Coral Reefs* **29**, 649–659.
- Naumann, M. S., Orejas, C., Wild, C. and Ferrier-Pagès, C. (2011). First evidence for zooplankton feeding sustaining key physiological processes in a scleractinian cold-water coral. *J. Exp. Biol.* **214**, 3570–3576.
- Naumann, M. S., Orejas, C. and Ferrier-Pagès, C. (2013a). High thermal tolerance of two Mediterranean cold-water coral species maintained in aquaria. *Coral Reefs* **32**, 749–754.
- Naumann, M. S., Orejas, C. and Ferrier-Pagès, C. (2013b). Species-specific physiological response by the cold-water corals *Lophelia pertusa* and *Madrepora oculata* to variations within their natural temperature range. *Deep Sea Res. Part 2 Top. Stud. Oceanogr.* **99**, 36–41.
- Orr, J. C., Fabry, V. J., Aumont, O., Bopp, L., Doney, S. C., Feely, R. A., Gnanadesikan, A., Gruber, N., Ishida, A., Joos, F. et al. (2005). Anthropogenic ocean acidification over the twenty-first century and its impact on calcifying organisms. *Nature* **437**, 681–686.
- Palmiéri, J., Orr, J. C., Dutay, J.-C., Béranger, K., Schneider, A., Beuvier, J. and Somot, S. (2015). Simulated anthropogenic CO₂ storage and acidification of the Mediterranean Sea. *Biogeosciences* **12**, 781–802.
- Purser, A., Larsson, A. I., Thomsen, L. and van Oevelen, D. (2010). The influence of flow velocity and food concentration on *Lophelia pertusa* (Scleractinia) zooplankton capture rates. *J. Exp. Mar. Biol. Ecol.* **395**, 55–62.
- Raddatz, J., Rüggeberg, A., Flögel, S., Hathorne, E. C., Liebetrau, V., Eisenhauer, A. and Dullo, W.-C. (2014). The influence of seawater pH on U / Ca ratios in the scleractinian cold-water coral *Lophelia pertusa*. *Biogeosciences* **11**, 1863–1871.
- Ries, J. (2011a). Acid ocean cover up. *Nat. Clim. Change* **1**, 294–295.
- Ries, J. B. (2011b). Skeletal mineralogy in a high-CO₂ world. *J. Exp. Mar. Biol. Ecol.* **403**, 54–64.
- Roberts, J. M., Wheeler, A. J. and Freiwald, A. (2006). Reefs of the deep: The biology and geology of cold-water coral ecosystems. *Science* **312**, 543–547.
- Rodolfo-Metalpa, R., Montagna, P., Aliani, S., Borghini, M., Canese, S., Hall-Spencer, J. M., Foggo, A., Milazzo, M., Taviani, M. and Houlbrèque, F. (2015). Calcification is not the Achilles' heel of cold-water corals in an acidifying ocean. *Glob. Change Biol.* **21**, 2238–2248.
- Thresher, R. E., Tilbrook, B., Fallon, S., Wilson, N. C. and Adkins, J. (2011). Effects of chronic low carbonate saturation levels on the distribution, growth and skeletal chemistry of deep-sea corals and other seamount megabenthos. *Mar. Ecol. Prog. Ser.* **442**, 87–99.
- Tremblay, P., Naumann, M. S., Sikorski, S., Grover, R. and Ferrier-Pagès, C. (2012). Experimental assessment of organic carbon fluxes in the scleractinian coral *Stylophora pistillata* during a thermal and photo stress event. *Mar. Ecol. Prog. Ser.* **453**, 63–77.
- Tsounis, G., Orejas, C., Reynaud, S., Gili, J.-M., Allemand, D. and Ferrier-Pagès, C. (2010). Prey-capture rates in four Mediterranean cold water corals. *Mar. Ecol. Prog. Ser.* **398**, 149–155.
- Turley, C. M., Roberts, J. M. and Guinotte, J. M. (2007). Corals in deep-water: will the unseen hand of ocean acidification destroy cold-water ecosystems? *Coral Reefs* **26**, 445–448.
- Tursi, A., Mastrototaro, F., Matarrese, A., Maiorano, P. and D'Onghia, G. (2004). Biodiversity of the white coral reefs in the Ionian Sea (Central Mediterranean). *Chem. Ecol.* **20** Suppl. 1, 107–116.
- Venn, A. A., Tambutté, E., Holcomb, M., Laurent, J., Allemand, D. and Tambutté, S. (2013). Impact of seawater acidification on pH at the tissue-skeleton interface and calcification in reef corals. *Proc. Natl. Acad. Sci. USA* **110**, 1634–1639.
- Walter, L. M. and Morse, J. W. (1985). The dissolution kinetics of shallow marine carbonates in seawater: a laboratory study. *Geochim. Cosmochim. Acta* **49**, 1503–1513.
- Weinbauer, M. G., Ogier, J. and Maier, C. (2012). Microbial abundance in the coelenteron and mucus of the cold-water coral *Lophelia pertusa* and in bottom water of the reef environment. *Aquat. Biol.* **16**, 209–216.
- Wijgerde, T., Silva, C. I. F., Scherders, V., van Bleijswijk, J. and Osinga, R. (2014). Coral calcification under daily oxygen saturation and pH dynamics reveals the important role of oxygen. *Biol. Open* **3**, 489–493.
- Wild, C., Huettel, M., Klüeter, A., Kremb, S. G., Rasheed, M. Y. M. and Jørgensen, B. B. (2004a). Coral mucus functions as an energy carrier and particle trap in the reef ecosystem. *Nature* **428**, 66–70.
- Wild, C., Rasheed, M., Werner, U., Franke, U., Johnstone, R. and Huettel, M. (2004b). Degradation and mineralization of coral mucus in reef environments. *Mar. Ecol. Prog. Ser.* **267**, 159–171.
- Wild, C., Woyt, H. and Huettel, M. (2005). Influence of coral mucus on nutrient fluxes in carbonate sands. *Mar. Ecol. Prog. Ser.* **287**, 87–98.
- Wild, C., Mayr, C., Wehrmann, L., Schöttner, S., Naumann, M., Hoffmann, F. and Rapp, H. T. (2008). Organic matter release by cold water corals and its implication for fauna–microbe interaction. *Mar. Ecol. Prog. Ser.* **372**, 67–75.
- Wild, C., Wehrmann, L. M., Mayr, C., Schöttner, S. I., Allers, E. and Lundälv, T. (2009). Microbial degradation of cold-water coral-derived organic matter: potential implication for organic C cycling in the water column above Tisler Reef. *Aquat. Biol.* **7**, 71–80.
- Wooldridge, S. (2013). A new conceptual model of coral biomineralisation: Hypoxia as the physiological driver of skeletal extension. *Biogeosciences* **10**, 2867–2884.
- Zetsche, E.-M., Baussant, T., Meysman, F. J. R. and van Oevelen, D. (2016). Direct visualization of mucus production by the cold-water coral *Lophelia pertusa* with digital holographic microscopy. *PLoS ONE* **11**, e0146766.